

Crop height variability detection in a single field by multi-temporal terrestrial laser scanning

Dirk Hoffmeister¹ · Guido Waldhoff¹ · Wolfgang Korres¹ ·
Constanze Curdt¹ · Georg Bareth¹

Published online: 29 October 2015
© Springer Science+Business Media New York 2015

Abstract Information on crop height, crop growth and biomass distribution is important for crop management and environmental modelling. For the determination of these parameters, terrestrial laser scanning in combination with real-time kinematic GPS (RTK–GPS) measurements was conducted in a multi-temporal approach in two consecutive years within a single field. Therefore, a time-of-flight laser scanner was mounted on a tripod. For georeferencing of the point clouds, all eight to nine positions of the laser scanner and several reflective targets were measured by RTK–GPS. The surveys were carried out three to four times during the growing periods of 2008 (sugar-beet) and 2009 (mainly winter barley). Crop surface models were established for every survey date with a horizontal resolution of 1 m, which can be used to derive maps of plant height and plant growth. The detected crop heights were consistent with observations from panoramic images and manual measurements ($R^2 = 0.53$, RMSE = 0.1 m). Topographic and soil parameters were used for statistical analysis of the detected variability of crop height and significant correlations were found. Regression analysis ($R^2 < 0.31$) emphasized the uncertainty of basic relations between the selected parameters and crop height variability within one field. Likewise, these patterns compared with the normalized difference vegetation index (NDVI) derived from satellite imagery show only minor significant correlations ($r < 0.44$).

Keywords Terrestrial laser scanning · RTK–GPS · Crop surface models · Spatial variability · Crop height

✉ Dirk Hoffmeister
dirk.hoffmeister@uni-koeln.de

¹ Institute of Geography, University of Cologne, Albertus-Magnus-Platz, 50923 Cologne, Germany

Introduction

Crop height, crop growth and biomass distribution are important parameters for precision agriculture (PA) and environmental modelling. Generally, crops are influenced by management, topography, diseases, soil and weather (Kravchenko et al. 2005). The quantification of the effects from these numerous and very variable factors affecting yield can be carried out by statistical analysis of yield (Heuer et al. 2011; Kravchenko et al. 2005; McKinion et al. 2010b). Kaspar et al. (2003) found in a 6 year corn dataset that corn yield is correlated to topographic factors, which were established from a kinematic DGPS survey. In this case, in years with lower precipitation, the well-known effect of higher yields in low lying areas, which benefit from moisture and better soil properties, can be proven. However, in years with high precipitation or strong precipitation events, the pattern is reversed. This knowledge facilitates the establishment of yield stability maps, which can be used to adjust management (McKinion et al. 2010b).

In contrast to the approaches mentioned that use yield data, also the current status of crop height, density, vitality and biomass is important for PA (Mulla 2013). For instance, information about plant vitality and biomass can be obtained by multi- and hyperspectral remote sensing (Gnyp et al. 2013; Yu et al. 2013). Further methods to gather data on the spatial distribution of crop height and other parameters are photogrammetric approaches carried out from unmanned airborne vehicles (UAVs) (Bendig et al. 2013; Gómez-Candón et al. 2013; Samseemoung et al. 2012), or balloons (Murakami et al. 2012), as well as radar remote sensing (Koppe et al. 2013). The distribution of plant height and a relation to biomass is important for the calculation of the nitrogen nutrition index (NNI), which enables determination of the ideal amount of N (Bendig et al. 2014).

Laser scanning, which is based on light detection and ranging (LIDAR), has also been applied in agronomy. It provides highly accurate and dense 3D point measurements of objects. The systems can be used at different scales, areas and accuracies. The technology can be used on airborne platforms, known as airborne laser scanning (ALS), on mobile platforms, known as mobile laser scanning (MLS), as well as on terrestrial platforms, known as terrestrial laser scanning (TLS). Various application areas, like topographic surveys, forestry and documentation of buildings and cultural heritage have been reported (Vosselman and Maas 2010).

For the detection of crop structure and other parameters, this method has been used by several authors. Ehlert et al. (2008) tested a laser scanner at different viewing angles on field machinery to directly derive data on crop height, coverage and density and found correlations between crop height, fresh and dry biomass of oilseed rape, winter rye, winter wheat and grassland ($R^2 > 0.88$). Lumme et al. (2008) investigated crop heights of differently fertilized barley, oats and wheat plots with a phase-based-scanner mounted on a 3 m rack. A correlation between crop height and grain yield was reported and single ears were successfully detected ($R^2 > 0.88$). Hosoi and Omasa (2009) used a triangulation-based scanner for the voxel-based estimation of plant area density, leaf area density and leaf area index of wheat ($R^2 > 0.9$). The approach was successfully transferred to rice by implementing a mirror above the canopy to accurately estimate the previously stated parameters (Hosoi and Omasa 2012). Crop structure and the associated chlorophyll content can be derived by the integration of intensity values of a green laser, which are radiometrically corrected (Eitel et al. 2010). Moreover, the nitrogen status in young wheat canopies can also be derived with this approach (Eitel et al. 2011). Höfle (2014) presented an approach to use corrected intensity values for the discrimination of single maize plants.

In contrast to the already mentioned approaches, an indirect multi-temporal approach for the determination of the spatial distribution of crop height and crop growth of an entire, normally managed field was applied in this study. Sugar-beet was planted in 2008 and barley in 2009. In all cases, maps of crop height and crop growth were established by a comparison of high-resolution, multi-temporal crop surface models (CSMs) from different time steps (Hoffmeister et al. 2010). The aim of this study, in contrast to the previously described statistical studies on yield, is to find factors for the derived crop height and crop growth patterns by statistical analysis with topographic and soil parameters. In addition, comparisons with the normalized difference vegetation index (NDVI) derived from satellite imagery was used to prove the importance of these measurements.

Materials and methods

Project and site description

The study was applied within the framework of the Transregional Collaborative Research Centre 32 (CRC/TR32) “Patterns in Soil-Vegetation-Atmosphere-Systems”, which is an interdisciplinary research project, focusing on exchange processes between the soil, vegetation and the adjacent atmospheric boundary layer. The overall research goal of the CRC/TR32 is to yield improved numerical SVA models to predict CO₂, water and energy transfer by calculating patterns at various spatial and temporal scales. The focus is on the catchment area of the river Rur, situated in western Germany, parts of Belgium, and the Netherlands (CRC/TR32 2015).

The study was conducted on a single field (Fig. 1), which was intensively observed by different sensors for research issues of the CRC/TR32 (Korres et al. 2010; Koyama et al. 2010; Waldhoff et al. 2012; Schmidt et al. 2012). The field (N50°51'58", E6°26'50") is situated in an intensively used agricultural area, located about 40 km to the west of Cologne, Germany. It is around 405 m by 105 m with an area of about 4.3 ha, an elevation of 102–105 m above sea level and has gentle slopes (<2.5°). The soil of the study field is heterogeneous in terms of soil type distribution. The two most abundant soil types are a gleyic Luvisol in the west changing to a gleyic Cambisol in the east. In addition, some areas with anthropogenic soils (filled or removed

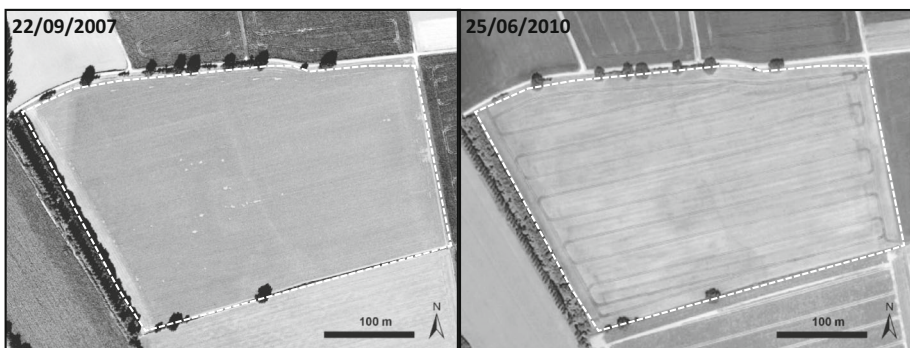


Fig. 1 Orthophotos of the observed field (white dashed line) from two different years showing the in-field variability of crops. Imagery (left): © Geobasis NRW 2007. Imagery (right): © 2012 Google, Digital Globe, 25.06.2010

material) have been identified in the middle part. In 2008, sugar-beet was planted followed by winter barley flanked by two strips of winter wheat in 2009.

TLS and RTK–DGPS surveys

A laser scanner (LMS-Z420i, Riegl, Horn, Austria) was used for all observations. In addition, a high-resolution digital camera, Nikon D200, was mounted on the head of the laser scanner for taking pictures, which were used to colour the point clouds. The different positions of the laser scanner were measured by a highly accurate real-time kinematic GPS (RTK-GPS) (HiPer Pro, Topcon, Tokyo, Japan). The relative accuracy of this device is ~ 10 mm in regard to the base station that was established above a marked point every time. The marked point was translated into the state surveying network by using six surrounding survey points within a 2 km distance (Seeber 2003). To estimate the direction of the point cloud and as a first estimation for the orientation of each point cloud from each scan position and date, several highly reflective targets mounted on ranging poles (reflectors) were additionally measured by the RTK–GPS and the TLS (Hoffmeister et al. 2010). The laser scanner was mounted on a tripod at a height of >1.5 m. To cover the entire area, eight scan positions were established in 2008 and one further scan position was added in 2009. Measurements were undertaken three times in 2008 (14/05/08, 26/06/08, 24/07/08) and four times in 2009 (07/04/09, 18/05/09, 24/06/09, 20/07/09) during the growing seasons. Each first date was used to establish the initial digital terrain model (DTM).

Post-processing

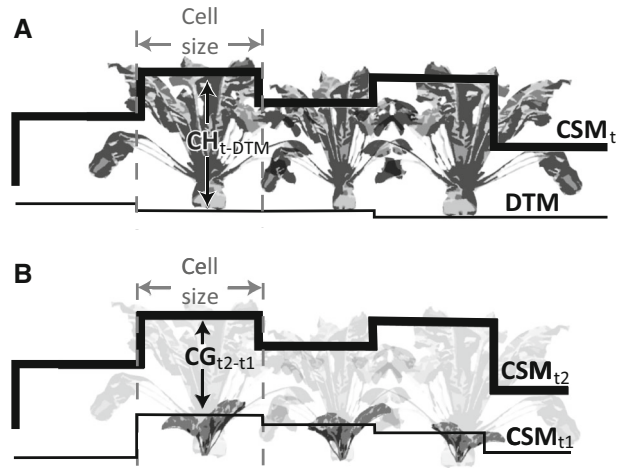
The registration of each scan position was facilitated by georeferencing every point cloud. For this purpose, the RTK–GPS measurements of each position of the laser scanner and one reflector for orientation were used. The iterative closest point (ICP)-algorithm (Besl and McKay 1992), which is implemented in the scanner's software as multi-station adjustment (MSA) enhanced the registration by iteratively minimizing differences of points (Vosselman and Maas 2010). The colourisation of each point within the point clouds was possible by assigning the RGB-values of the pictures taken by the digital camera. The area of interest was manually extracted and filtered in several steps. The point clouds containing ~ 10 million points were finally interpolated with the same resolution of 1 m by inverse distance weighting (IDW) to establish the initial DTM and the CSMs representing the top canopy of every other survey. To determine the crop height (CH), a CSM of a certain time step (t) was compared to the initial DTM from the first measurement before crop emergence, as depicted in Eq. 1 and shown in Fig. 2a.

$$CH = CSM_t - DTM \quad (1)$$

The resulting CH depicts the current, absolute crop height of the assigned survey date. The results are visually controlled by the corresponding panoramic pictures of the mounted camera and are evaluated with the manual measurements of plant height by comparing mean values of the CSM (1 m^2) at the position of the measurement. In contrast, crop growth (CG) can be established by comparing two CSMs from successive dates to retrieve the relative crop growth between those dates, as defined by Eq. 2 and depicted in Fig. 2b.

$$CG = CSM_{t_2} - CSM_{t_1} \quad (2)$$

Fig. 2 Illustration of the derivation of crop height (CH) by comparison of CSMs and the initial DTM (a). Crop growth (CG) is derived by a comparison of two consecutive CSMs (b)



In-situ crop analysis and biomass harvesting

Manual crop height measurements at 27 locations and biomass harvesting at three of these locations was conducted every 2 weeks within the first year. Manual measurements of crop height at each spot were conducted at three plants with a measuring tape. Biomass was extracted from three plants representing an area of 0.5 by 0.5 m at each spot. The cleaned leaves were dried for 3 days at a temperature of 105 °C, weighed and an average dry biomass in g m^{-2} was calculated.

Soil data

Soil moisture measurements, reported as the ratio of water and soil volume (vol. %), were made with a handheld FDR probe (Delta-T Devices Ltd., Cambridge, UK) at 24 points on a 50 by 50 m grid (Korres et al. 2010). The mean of six measurements for each point at the dates, listed in Table 1, were interpolated by inverse distance weighting. Mean soil depth and the soil score were digitized from the corresponding soil maps of the State's geological agency. The soil score has a value of zero to one hundred and should represent soil fertility derived from the soil composition, geologic origin and current condition and altered by local climatic and topographic variations. Soil depth and soil score values were mapped at a scale of 1:5000 established by ground surveys of federal agencies.

Correlation and regression analysis

The measured DTM was validated by a DTM from the state's surveying agency generated by ALS at a 1 m resolution (DGM1L). The CH and CG values averaged over 1 m^2 were compared with manual crop height and biomass measurements. In order to analyze factors that might have influenced variability of crop height and crop growth, different parameters were derived from the DTM with different cell sizes (1, 5, 10, 20 m). These parameters were the absolute height, slope, curvature, plan and profile curvature of the terrain, as well

Table 1 Parameters incorporated for analysis of the detected variability of CH and CG

Parameter	Description
Height	Z values of the DTM derived from the first measurements of every year
Slope	Slope is the maximum degree of change between each cell and its neighbours
Curvature	Curvature is the gradient of the slope. Positive numbers depict convex curvatures, negative values show concave curvatures, zero values are flat
Plan curvature	Plan curvature is perpendicular to the direction of the maximum slope. Positive values assign sidewardly convex surfaces and negative values denote sidewardly concave surfaces. Zero values are denoted for linear surfaces
Profile curvature	Profile curvature is in the direction of the maximum slope. A negative value assigns an upwardly convex surface and likewise a positive value indicates a concave surface. Zero values are denoted for linear surfaces
Soil moisture	Mean values of measured data from specified date (08/07/2008, 25/07/2008, 07/08/2009), interpolated by inverse distance weighting
Soil depth	Mean soil depth in decimetre from the soil map
Soil score	Soil score from the soil map

as soil moisture, soil depth and soil score (Table 1). Slope and curvature values were derived by ArcGIS for Desktop (ESRI, Redlands, USA) (Longley et al. 2006). The parameters derived from the DTM (slope and curvature values) were separately derived from the DTM with the corresponding cell size.

In addition, the principal components from the crop height data for the 2 years were calculated with a principal component analysis (PCA). For this procedure, the data for each measurement date was standardized to a zero mean and a standard deviation of one to ensure a uniformly weighted contribution of every date to the principal components (Korres et al. 2010). With this single parameter PCA, the stable patterns of crop height were calculated for the years 2008 and 2009 and entered into the correlation analysis.

For the statistical evaluation of the crop height and crop growth variability, center points from the DTM raster data were established for each cell and all data were attributed to these points. Generally, a bi-linear interpolation function was used to derive values for each point at each resolution. Finally, attribute tables of these point data, such as mean plant height, slope value and soil moisture, were exported for each resolution and used for correlation and regression analysis in R-statistical software. For tests on statistical significance, spatial auto-correlation was determined by modified *t* tests in the PASSAGE 2 software (Taylor and Bates 2013).

Evaluation with satellite imagery

The detected crop height variability could be (in terms of modelling approaches) of interest for the entire region. Parameters derived from satellite imagery were compared to the resulting crop height and crop growth distribution. Images from the ‘Advanced Spaceborne Thermal Emission and Reflection Radiometer’ (ASTER), Landsat (TM/ETM+) and RapidEye satellites were used. Acquisition dates, raster resolution and bands used for NDVI calculation are listed in Table 2. Likewise, the data were statistically evaluated, as stated before. In order to avoid mixed-pixel problems by surrounding trees, a surrounding buffer of 15 m was removed before analysis. Thus, only the inner field area was considered.

Table 2 Overview of incorporated satellite imagery, raster resolution and bands used for NDVI calculation

Satellite	Acquisition date	Resolution	Bands used
Landsat 7 (ETM+)	29/06/2008	30 m	Band 3 visible (red) (0.63–0.69 μm) 30 m and band 4 near-infrared (0.77–0.90 μm)
ASTER	24/07/2008	15 m	Band 2 red (0.63–0.69 μm) and band 3 near-infrared (0.76–0.86 μm)
RapidEye	24/05/2009	5 m	Band 3 red (630–685 nm) and band 5 near-infrared (760–850 nm)
ASTER	02/07/2009	15 m	Band 2 red (0.63–0.69 μm) and band 3 near-infrared (0.76–0.86 μm)

Results

Point clouds with an accuracy of about 10 mm were achieved as a primary result. Merging those point clouds of every single scan position was possible by the RTK–GPS measurements and enhancement by the MSA procedure with a RMSE < 10 mm. The DTM from the first date and the CSMs taken from the latter dates were generated by interpolation from the final point clouds with approximately 10 million single measurements. With regard to the point density distribution, which depends on the range, a 1 m cell size was chosen as the initial resolution.

Comparison of elevation models

The derived DTM ($\bar{X} = 103.53 \pm 0.53$ m) was compared to the DGM1L ($\bar{X} = 102.86 \pm 0.51$ m), which is distributed with an accuracy of 0.2 m obtained from the state's surveying agency to test the overall accuracy of the approach. A significant correlation ($r = 0.99$) was found that reveals the relative precision of the measurements. For the TLS measurements, a positive shift of ~ 0.8 m was observed.

Results of 2008 and accuracy analysis

The maps of crop height, crop growth, and the initial DTM from 2008 are presented in Fig. 3. Statistical values are shown in Table 3. Sugar-beet shows throughout the observation period an increase in plant height, with a larger standard deviation (SD ~ 0.1) and coefficient of variation (CV > 0.23). The generated DTM (Fig. 3a) shows the major topographic patterns of the field, which is characterized by an east to west downhill trend with several local depressions at the eastern and central parts, as well as a sharp linear edge in the central section. These overall patterns are reflected by the map of crop height from late June, 2008 (Fig. 3b). Particularly, the eastern central part and the whole western edge show inferior crop development. Furthermore, west of the linear edge, several distinctive, circular areas with different crop development can be observed (Fig. 3d). These patterns appear reversed in the maps of crop growth between late June and late July 2008 (Fig. 3c).

The low lying western part is generally characterized by inferior growth, as well as the small depression in the central eastern part. A panoramic picture generated from the camera on the TLS (Fig. 4) from the last survey of 2008 shows the poorer development of the sugar-beet plants on the western side. In Fig. 3d, the mainly covered area of the picture

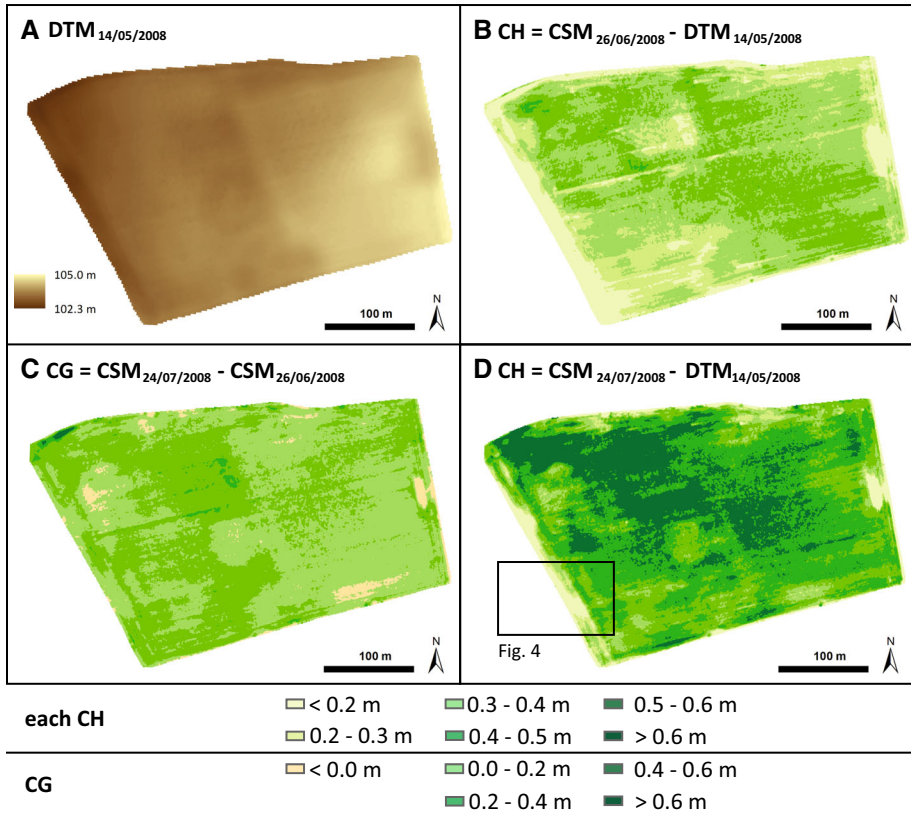


Fig. 3 Maps of crop height (CH), crop growth (CG) and the DTM for the year 2008. CH and CG were determined by a comparison of consecutive CSMs and the DTM. *Rectangle* marks the area of a panoramic picture for the corresponding survey date (Fig. 4)

Table 3 Overview of the derived crop height and crop growth values (n = 983), as well as manually measured crop heights (n = 27) in meters for 2008 (Fig. 3) and 2009 (Fig. 5)

		Derived values			Measured values	
		\bar{X}	SD	CV	\bar{X}	SD
Sugar beet 2008	CH 080624–080525	0.33	0.11	0.33	0.34	0.10
	CH 080725–080525	0.52	0.12	0.23	0.52	0.12
	CG 080725–080624	0.19	0.09			
Barley and wheat 2009	CH 090518–090418	0.80	0.06	0.08		
	CH 090624–090418	0.98	0.08	0.08		
	CH 090720–090418	0.83	0.08	0.10		
	CG 090624–090518	0.18	0.06			
	CG 090720–090624	-0.16	0.05			

CV coefficient of variation



Fig. 4 Panoramic picture from one scan position from 24 July 2008. The western part of the field showing inferior growth is visible in the foreground. The area is marked in Fig. 3

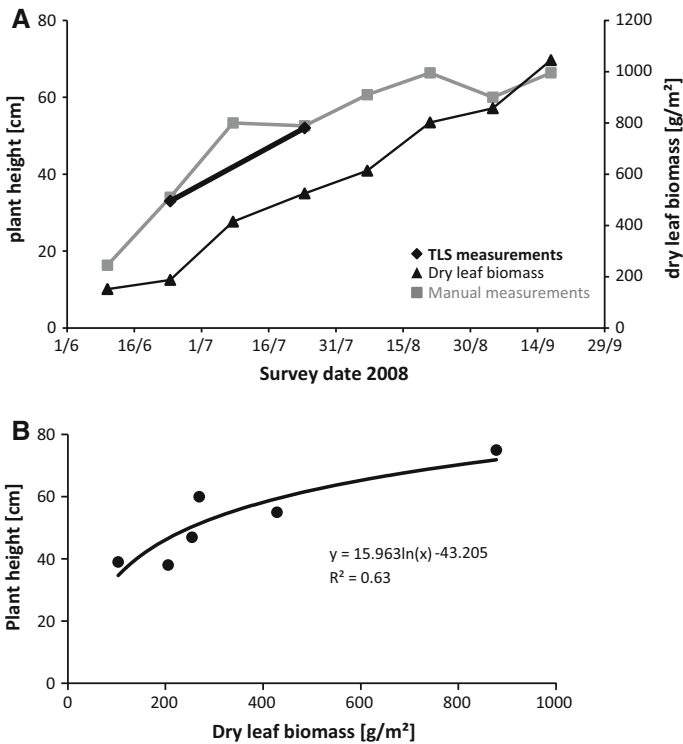


Fig. 5 Comparison of the manually measured crop heights and dry leaf biomass of the whole vegetation period of 2008 (a) with the derived, mean crop height values ($n = 27$). Three of these locations were used for biomass extraction and used in a linear regression with dry leaf biomass (b)

is marked. Generally, all observations match with the pictures and manual measurements of crop height. The calculated plant heights of the CSMs were compared with independent crop height measurements on the field for the year 2008. The manual measurements were in agreement with the derived plant height values as depicted in Table 3 and the R^2 is 0.53. RMSE is 0.1, which equals to a relative error of 22 %.

In addition, biomass sampling of sugar-beet plants was conducted in 2008 at three points within the field. Biomass and plant height for the whole growing period are shown in Fig. 5a, with the mean crop height of the TLS measurements. Assuming a logarithmic regression (Fig. 5b), R^2 value was 0.63. Generally, the quantity of the independent crop height measurements is low.

Results of 2009

Barley and wheat exhibited a more uniform crop height and crop growth than sugar-beet in 2008. This is reflected by a minor SD (<0.1) and CV (<0.1). The pattern of the initial DTM is not visually recognizable. Inferior crop development of barley was detected only for the north-western part. In late July, the crop height generally decreased, close to harvest, due to ear development. This is also seen in the mostly negative crop development between late June and late July (Fig. 6f). The narrow strips of wheat show slightly different crop heights at certain time steps (e.g., Fig. 6d). Statistical values are given in Table 3.

Correlation between crop height variation and selected parameters

The detected variability of crop height and crop growth was compared to the previously stated parameters, in order to identify sources for this crop height variation. The mean plant heights were correlated with the stated parameters in R-statistical software with a resolution of 1, 5, 10 and 20 m respectively. Significant parameters were used in a multiple, linear regression in order to explain this variation. The results for the resolution of the 10 m cell size showed in this case the best results and are listed in Table 4 ($n = 983$). Similar but lower correlation values were derived for the chosen resolutions. Generally, correlation coefficients were low (<0.4), and significance is mostly reduced, concerning spatial autocorrelation. Significant correlations of slope, curvature, plan and profile curvature, as well as for the soil depth were found for sugar-beet in 2008. Here, slope and profile curvature are negatively correlated. Only minor correlations for all curvatures are indicated for crop growth in 2008. For 2009, curvature was negatively correlated, whereas profile curvature was positively correlated. For the latest stage in 2009 soil depth was additionally correlated ($r = 0.38$) For crop growth, slope and soil moisture showed a correlation with the first growing period from May to late June of 2009, whereas for the second growing period only soil depth was correlated. Significant parameters were used in a multiple linear regression computation for every CH and CG stage. The R^2 values were generally low (<0.29) and only a part of the crop height distribution of 2008 is related to the selected parameters. For 2009, the coefficients of determination were negligible.

In order to derive a generalized statement, the principal components of crop height for each year were computed. The main annual patterns are depicted by the first principal component (PC1) and the variation is reflected by the second principal component (PC2). For 2008, in PC1 slope was negatively correlated to crop height and positively correlated to variation. Likewise, profile curvature was positively correlated to this variation. In contrast, curvature, plan curvature and soil depth were negatively correlated to PC2, which are values that are positively correlated to plant height. In 2009, slope was correlated to the variation reflected by PC2 (0.21). Curvature (-0.18) and profile curvature (0.21) were significantly correlated to PC1.

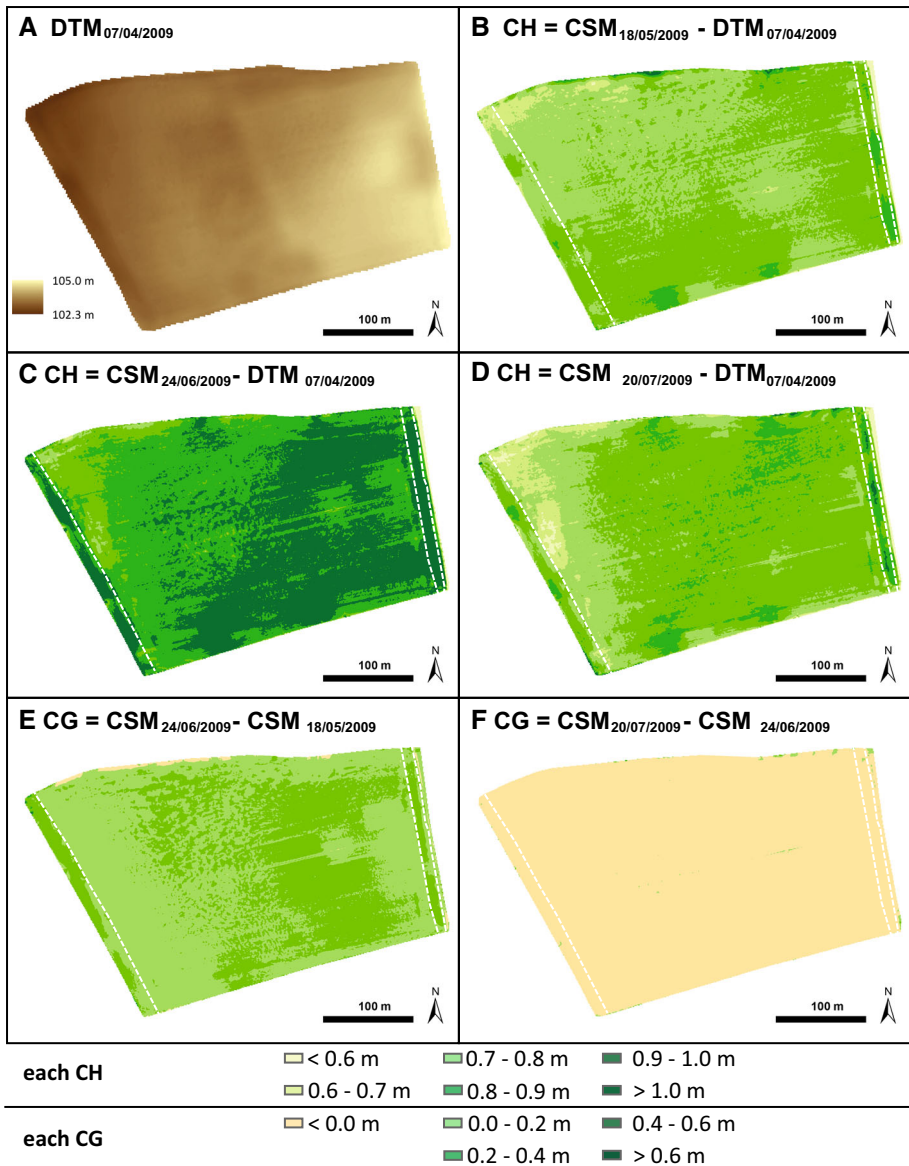


Fig. 6 Maps of crop height (CH), crop growth (CG) and the DTM for the year 2009. CH and CG were determined by a comparison of consecutive CSMs and the DTM. The main crop was winter barley with two narrow areas of winter wheat, which are marked by *white dashed lines*

In Table 5, the results of the comparison between the derived crop height and crop growth values and the computed NDVI from satellite imagery are shown. Significant correlations of ~ 0.35 were only found for sugar-beet crop height variation in 2008 and crop growth of the first period in 2009 ($r = 0.44$).

Table 4 Derived correlation coefficients r of the comparison between crop height (CH) and crop growth (CG) and selected parameters

	n = 983	Height	Slope	Curvature	Plan curvature	Profile curvature	Soil moisture	Soil depth	Soil score	Multi. lin. regression (adj. R^2)
Sugar-beet 2008	CH 080624–080525	0.24 ^b	-0.31 ^a	0.33 ^a	0.31 ^a	-0.26 ^a	-0.01	0.40 ^a	0.19	0.29
	CH 080725–080525	-0.01	-0.28 ^a	0.22 ^a	0.21 ^a	-0.17 ^a	0.22	0.22 ^a	0.02	0.14
	CG 080725–080624	-0.28 ^b	-0.01	-0.09 ^a	-0.07 ^a	0.08 ^a	0.16	-0.16	-0.19	0.00
Barley and wheat 2009	PC1 2008 (77 %)	-0.16 ^b	-0.17 ^a	0.07 ^a	0.08 ^a	-0.05	0.17 ^b	0.03	-0.10 ^b	0.03
	PC2 2008 (23 %)	-0.29 ^b	0.28 ^a	-0.30 ^a	-0.32 ^a	0.26 ^a	0.05	-0.40 ^a	-0.22 ^b	0.27
Barley and wheat 2009	CH 090518–090418	0.25 ^b	0.09 ^b	-0.16 ^a	-0.07 ^b	0.19 ^a	-0.07	0.18	0.10	0.02
	CH 090624–090418	0.30 ^b	-0.09 ^b	-0.18 ^a	-0.08 ^b	0.21 ^a	0.09	0.23	0.19	0.03
	CH 090720–090418	0.29 ^b	-0.10 ^b	-0.14 ^a	-0.04	0.18 ^a	0.12	0.38 ^a	0.17	0.04
Barley and wheat 2009	CG 090624–090518	0.13 ^b	-0.19 ^a	-0.06	-0.04	0.07 ^b	0.17 ^a	0.11	0.13	0.05
	CG 090720–090624	0.00	-0.02	0.04	0.07 ^b	-0.02	0.04	0.29 ^a	-0.01	0.08
Barley and wheat 2009	PC1 2009 (80 %)	0.31 ^b	-0.04	-0.18 ^a	-0.07 ^b	0.21 ^a	0.06	0.29 ^b	0.18 ^b	0.03
	PC2 2009 (15 %)	-0.02	0.21 ^a	-0.03	-0.02	0.02	-0.21 ^a	-0.12 ^b	-0.07 ^b	0.07

Adjusted R^2 values from multiple linear regression analysis of significant values. Main annual patterns are revealed by the first principle component (PC1), the variability is represented by the second (PC2)

Two-tailed modified t test of significance is used

^a Correlation is significant at the 0.05 level

^b Significance is reduced by modified t test

Table 5 Derived correlation coefficients r of the comparison between crop height (CH) and crop growth (CG) and the NDVI from different satellite images

	n = 983	NDVI 080629	NDVI 080724	NDVI 090524	NDVI 090702
Sugar-beet 2008	CH 080624–080525	0.35 ^a			
	CH 080725–080525		0.36 ^a		
	CG 080725–080624	−0.15 ^b	0.09 ^b		
Barley and wheat 2009	CH 090518–090418			0.12 ^b	
	CH 090624–090418				0.48 ^b
	CH 090720–090418				0.51 ^b
	CG 090624–090518			0.44 ^a	0.41 ^b
	CG 090720–090624			0.17 ^b	0.15 ^b

Two-tailed modified t test of significance is used

^a Correlation is significant at the 0.05 level

^b Significance is reduced by modified t test

Discussion

Considering the method itself, the system and all components worked well. Surveys cannot be conducted during rain, as most instruments are only splash proof. Dust and insects caused some noise. The georeferencing approach of combining TLS surveys with accurate RTK–GPS measurements made an analysis and comparison with other georeferenced data possible. This was of particular importance in this study, as other data were incorporated to determine factors for crop height and crop growth variation. For this purpose, the RTK–GPS base station was transformed into the state surveying network. The comparison with the DTM of the state surveying agency revealed a shift of about 0.8 m, which might be the result of different measurement methods and following post-processing steps. McKinion et al. (2010a) found comparable results (± 1 m). However, the relative relationship here shows a high correlation, which confirms the general accuracy of this approach.

The resulting point density of the TLS surveys needs to be taken into consideration. The surveys of the single field conducted with a tripod of 1.5 m height revealed a lower point density at a distance of ~ 100 m away from each scan position. Although an additional position was established in 2009 within the field, a full coverage with a high point density was still not achieved. Generally, less than 5 pts/m² were obtained. Compared to the surveys conducted with a tripod, an elevated position of ~ 4 m (Hoffmeister et al. 2012; Höfle 2014) resulted in a higher point density, which enables for instance single plant detection.

The method can be applied with a higher temporal resolution depending on organisation and logistics. However, the measurement time of about half a day for a field is a major disadvantage. An expansion to an MLS approach by incorporating an inertial navigation system (INS) would enable faster measurements with a more uniform and higher spatial and temporal resolution. Similarly, stereo-photogrammetry by UAVs (Bendig et al. 2013) could be applied to obtain more accurate and higher spatial and temporal resolution. However, this approach relies on ambient illumination, calmer weather conditions and the

placement of ground control points within the mapped area (Gómez-Candón et al. 2013). TLS and MLS are based on active sensors which are less prone to the ambient conditions.

In the TLS approach, the height of the plants was indirectly derived by a comparison over time. In contrast, the MLS described by Ehlert et al. (2009) involved a height guiding device in front of a carrier that holds the laser sensor at a constant height above the ground. This allowed the plant height to be computed by geometric relations. Lumme et al. (2008) mounted a phase-based scanner vertically on a 3 m rack. The resulting data was correlated by an indirect registration of plastic discs, measured by a tachymeter. Thus, in both cases, the crop height was directly measured.

However, direct comparison with manually measured crop heights showed the accuracy of the TLS approach (Table 3). In this study, the number of manual measurements were sparse. A similar set-up and procedure with more ground control was applied by Tilly et al. (2014) to paddy rice fields and revealed a high correlation between manual measurements and mean crop height values. Ehlert et al. (2009) found high correlations in his MLS approach for several crops. Their study did not include sugar beet. The correlation between sugar-beet height obtained manually and by TLS in this study were slightly worse, probably due to the more complex plant structure and the greater uncertainty in the manual crop height measurement. The derived crop height was a mean value of the corresponding cell size, whereas the manual measurement was here a subjectively chosen spot height, which might be biased.

Overall, the western part of the site showed poor crop development and the patterns were also visible in the orthophotos from years before and after the observations (Fig. 1). The north–south line in the centre of the site are the remains of old pathways, which existed prior to land reallocation. In addition, the whole area is shaped by an inactive palaeo-river system and remains of trenches and bomb craters from World War II (Rudolph et al. 2015 and personal communication, 2014), which might be the cause for the circular pattern in the middle of the field. The latter area is also denoted in the soil map as a cultural deposit or alteration area.

For correlation purposes, all data were aggregated to raster datasets of 1, 5, 10 and 20 m pixel resolution and compared to parameters from topography, soil information and soil moisture. The results of the 10 m resolution are presented here. Generally, only small significant correlation values were found ($r < 0.4$) and the applied modified t test has diminished several previously significant values. Similar small values were found in other studies concerning yield data (Heuer et al. 2011; McKinion et al. 2010b). For instance, McKinion et al. (2010b), related yield data from 5 years to topographic parameters and found regression values smaller than 0.11. In this case, slope, all curvature values and soil depth were correlated to sugar-beet height, whereas only curvature and profile curvature were correlated to barley and wheat height in 2009. Slope generally was correlated to the variation reflected by the second principal component. Overall, the selected parameters did not provide a satisfactory explanation for the variation of the derived plant heights in regression analysis ($R^2 < 0.31$). Other processes are probably responsible for the detected variability, for instance, management or nutrient availability. Results may be improved by using other soil parameters such as soil electrical conductivity (EC) (Stadler et al. 2015; Rudolph et al. 2015).

The detected variability is valuable information for crop growth models that consider temporal processes (Lenz-Wiedemann et al. 2010; Korres et al. 2013). Likewise, the crop height distribution can be used as a further source for these models. Correlation with the NDVI derived from available satellite imagery gave only r values smaller than 0.44. A combination of measured plant height and NDVI derived from high-resolution satellite

imagery (e.g., Worldview2, 5 m/pixel) resulted in a coefficient of determination for biomass modeling of $R^2 > 0.6$ (Hütt et al. 2014).

Conclusion

TLS has been shown as a possible multi-temporal surveying method for deriving plant height distribution, plant growth and biomass. A small number of sparse manual measurements resulted in a $R^2 = 0.53$, $RMSE = 0.1$ m to derived crop height values. Based on the results, the spatial variability of crop height and crop growth can be determined in one single field for two different crops in two different years by the method of combining TLS and RTK–GPS in multi-temporal surveys. The detected variability was different for both crop types. Winter barley and wheat in 2009 showed a more uniform crop height and crop growth pattern than sugar-beet in 2008. Generally, significant correlations with common topographic parameters and soil values were found. However, these showed, similar to studies concerning yield data, hardly an explanation for the variation. Likewise, the NDVI of different satellite imagery showed only a minor correlation. Thus, crop height, crop growth and biomass distribution are barely related to the selected parameters, which emphasizes the importance of these measurements in particular for modelling approaches.

Acknowledgments We thank the anonymous reviewers, who significantly improved the paper. We gratefully acknowledge financial support from the CRC/TR32, funded by the Deutsche Forschungsgemeinschaft (DFG). We also like to thank Topcon GmbH (Germany) and RIEGL Laser Measurement Systems GmbH (Austria) for continuous support.

Compliance with Ethical Standards

Conflict of interest We declare no conflict of interest.

References

- Bendig, J., Bolten, A., & Bareth, G. (2013). UAV-based imaging for multi-temporal, very high resolution crop surface models to monitor crop growth variability. *Photogrammetrie-Fernerkundung-Geoinformation*, 6, 551–562.
- Bendig, J., Bolten, A., Bennertz, S., Broscheit, J., Eichfuss, S., & Bareth, G. (2014). Estimating biomass of Barley using crop surface models (CSMs) derived from UAV-based RGB imaging. *Remote Sensing*, 6(11), 10395–10412.
- Besl, P. J., & McKay, N. D. (1992). A method for registration of 3-D shapes. *IEEE Transactions on Pattern Analysis and Machine Intelligence*, 14(2), 239–256.
- CRC/TR32 (2015). transregional collaborative research centre 32: Patterns in soil-vegetation-atmosphere-systems. Retrieved July 24, 2015, from <http://www.tr32.uni-koeln.de>.
- Ehlert, D., Adamek, R., & Horn, H.-J. (2009). Laser rangefinder-based measuring of crop biomass under field conditions. *Precision Agriculture*, 10(5), 395–408.
- Ehlert, D., Horn, H. J., & Adamek, R. (2008). Measuring crop biomass density by laser triangulation. *Computers and Electronics in Agriculture*, 61(2), 117–125.
- Eitel, J. U. H., Vierling, L. A., & Long, D. S. (2010). Simultaneous measurements of plant structure and chlorophyll content in broadleaf saplings with a terrestrial laser scanner. *Remote Sensing of Environment*, 114(10), 2229–2237.
- Eitel, J. U. H., Vierling, L. A., Long, D. S., & Hunt, E. R. (2011). Early season remote sensing of wheat nitrogen status using a green scanning laser. *Agricultural and Forest Meteorology*, 151(10), 1338–1345.
- Gnyp, M. L., Yu, K., Aasen, H., Yao, Y., Huang, S., Miao, Y., et al. (2013). Analysis of Crop Reflectance for Estimating Biomass in Rice Canopies at Different Phenological Stages. *Photogrammetrie-Fernerkundung-Geoinformation*, 2013(4), 351–365.

- Gómez-Candón, D., De Castro, A. I., & López-Granados, F. (2013). Assessing the accuracy of mosaics from unmanned aerial vehicle (UAV) imagery for precision agriculture purposes in wheat. *Precision Agriculture*, *15*(1), 44–56.
- Heuer, A., Casper, M. C., & Herbst, M. (2011). Correlation of topography, soil properties and spatial variability of biomass: application of the self-organizing map method. *Zeitschrift für Geomorphologie, Supplementary Issues*, *55*(3), 169–178.
- Hoffmeister, D., Bolten, A., Curdt, C., Waldhoff, G., & Bareth, G. (2010). High resolution crop surface models (CSM) and crop volume models (CVM) on field level by terrestrial laser scanning. In H. Guo, & C. Wang (Eds.), *Proceedings of SPIE-7840, 6th International Symposium on Digital Earth: Models, Algorithms, and Virtual Reality*, 2010 (p. 78400E). Göttingen, Germany: Copernicus Publications.
- Hoffmeister, D., Tilly, N., Bendig, J., Curdt, C., & Bareth, G. (2012). Detection of crop growth variability of four sugar beet cultivars by multi-temporal terrestrial laser scanning. In M. Clasen, G. Fröhlich, H. Bernhardt, K. Hildebrand, & B. Theuvsen (Eds.), *Informationstechnologie für eine nachhaltige Landwirtschaft, 32. GIL Jahrestagung* (pp. 135–138). Bonn, Germany: Köllen Verlag.
- Höfle, B. (2014). Radiometric correction of terrestrial LiDAR point cloud data for individual maize plant detection. *IEEE Geoscience and Remote Sensing Letters*, *11*(1), 94–98.
- Hosoi, F., & Omasa, K. (2009). Estimating vertical plant area density profile and growth parameters of a wheat canopy at different growth stages using three-dimensional portable lidar imaging. *ISPRS Journal of Photogrammetry and Remote Sensing*, *64*(2), 151–158.
- Hosoi, F., & Omasa, K. (2012). Estimation of vertical plant area density profiles in a rice canopy at different growth stages by high-resolution portable scanning lidar with a lightweight mirror. *ISPRS Journal of Photogrammetry and Remote Sensing*, *74*, 11–19.
- Hütt, C., Schiedung, H., Tilly, N., & Bareth, G. (2014). Fusion of high resolution remote sensing images and terrestrial laser scanning for improved biomass estimation of maize. In F. Sunar, O. Altan, & M. Taberner (Eds.), *ISPRS Archives* (Vol. XL-7, pp. 101–108). Göttingen, Germany: Copernicus Publications.
- Kaspar, T. C., Colvin, T. S., Jaynes, D. B., Karlen, D. L., James, D. E., & Meek, D. W. (2003). Relationship between six years of corn yields and terrain attributes. *Precision Agriculture*, *4*, 87–101.
- Koppe, W., Gnyp, M. L., Hutt, C., Yao, Y. K., Miao, Y. X., Chen, X. P., et al. (2013). Rice monitoring with multi-temporal and dual-polarimetric TerraSAR-X data. *International Journal of Applied Earth Observation and Geoinformation*, *21*, 568–576.
- Korres, W., Koyama, C. N., Fiener, P., & Schneider, K. (2010). Analysis of surface soil moisture patterns in agricultural landscapes using empirical orthogonal functions. *Hydrology and Earth System Sciences*, *14*(5), 751–764.
- Korres, W., Reichenau, T. G., & Schneider, K. (2013). Patterns and scaling properties of surface soil moisture in an agricultural landscape: An ecohydrological modeling study. *Journal of Hydrology*, *498*, 89–102.
- Koyama, C. N., Korres, W., Fiener, P., & Schneider, K. (2010). Variability of surface soil moisture observed from multi-temporal C-band SAR and field data. *Vadose Zone Journal*, *9*(4), 1014–1024.
- Kravchenko, A. N., Robertson, G. P., Thelen, K. D., & Harwood, R. R. (2005). Management, topographical, and weather effects on spatial variability of crop grain yields. *Agronomy Journal*, *97*(2), 514–523.
- Lenz-Wiedemann, V. I. S., Klar, C. W., & Schneider, K. (2010). Development and test of a crop growth model for application within a Global Change decision support system. *Ecological Modelling*, *221*(2), 314–329.
- Longley, P. A., Goodchild, M. F., Maguire, D. J., & Rhind, D. W. (2006). *Geographic information systems and science*. West Sussex, UK: Wiley.
- Lumme, J., Karjalainen, M., Kaartinen, H., Kukko, A., Hyypää, J., Hyypää, H., et al. (2008). Terrestrial Laser Scanning of agricultural crops. In J. Chen, J. Jiang, & H.-G. Maas (Eds.), *ISPRS archives, Proceedings of the XXI. ISPRS Conference* (Vol. XXXVII Part B5, pp. 563–566). Göttingen, Germany: Copernicus Publications.
- McKinion, J. M., Willers, J. L., & Jenkins, J. N. (2010a). Comparing high density LIDAR and medium resolution GPS generated elevation data for predicting yield stability. *Computers and Electronics in Agriculture*, *74*(2), 244–249.
- McKinion, J. M., Willers, J. L., & Jenkins, J. N. (2010b). Spatial analyses to evaluate multi-crop yield stability for a field. *Computers and Electronics in Agriculture*, *70*(1), 187–198.
- Mulla, D. J. (2013). Twenty five years of remote sensing in precision agriculture: Key advances and remaining knowledge gaps. *Biosystems Engineering*, *114*(4), 358–371.
- Murakami, T., Yui, M., & Amaha, K. (2012). Canopy height measurement by photogrammetric analysis of aerial images: Application to buckwheat (*Fagopyrum esculentum* Moench) lodging evaluation. *Computers and Electronics in Agriculture*, *89*, 70–75.

- Rudolph, S., van der Kruk, J., von Hebel, C., Ali, M., Herbst, M., Montzka, C., et al. (2015). Linking satellite derived LAI patterns with subsoil heterogeneity using large-scale ground-based electromagnetic induction measurements. *Geoderma*, 241–242, 262–271.
- Samseemoung, G., Soni, P., Jayasuriya, H. P. W., & Salokhe, V. M. (2012). Application of low altitude remote sensing (LARS) platform for monitoring crop growth and weed infestation in a soybean plantation. *Precision Agriculture*, 13(6), 611–627.
- Schmidt, M., Reichenau, T. G., Fiener, P., & Schneider, K. (2012). The carbon budget of a winter wheat field: An eddy covariance analysis of seasonal and inter-annual variability. *Agricultural and Forest Meteorology*, 165, 114–126.
- Seeber, G. (2003). *Satellite geodesy*. Berlin, Germany: Walter de Gruyter.
- Stadler, A., Rudolph, S., Kupisch, M., Langensiepen, M., van der Kruk, J., & Ewert, F. (2015). Quantifying the effects of soil variability on crop growth using apparent soil electrical conductivity measurements. *European Journal of Agronomy*, 64, 8–20.
- Taylor, J. A., & Bates, T. R. (2013). A discussion on the significance associated with Pearson's correlation in precision agriculture studies. *Precision Agriculture*, 14(5), 558–564.
- Tilly, N., Hoffmeister, D., Cao, Q., Huang, S. Y., Lenz-Wiedemann, V., Miao, Y. X., et al. (2014). Multitemporal crop surface models: accurate plant height measurement and biomass estimation with terrestrial laser scanning in paddy rice. *Journal of Applied Remote Sensing*, 8(1), 083671.
- Vosselman, G., & Maas, H.-G. (Eds.). (2010). *Airborne and terrestrial laser scanning*. Dunbeath, UK: Whittles Publishing.
- Waldhoff, G., Curdt, C., Hoffmeister, D., & Bareth, G. (2012). Analysis of multitemporal and multisensor remote sensing data for crop rotation mapping. In M. Shortis, W. Wagner, & J. Hyypä (Eds.), *XXII ISPRS Congress, Technical Commission VII* (Vol. I-7, pp. 177–182). Göttingen, Germany: Copernicus Publications.
- Yu, K., Li, F., Gnyp, M. L., Miao, Y., Bareth, G., & Chen, X. (2013). Remotely detecting canopy nitrogen concentration and uptake of paddy rice in the Northeast China Plain. *ISPRS Journal of Photogrammetry and Remote Sensing*, 78, 102–115.